

Plasmonic interaction between nanospheres

S. Yu and H. Ammari

Research Report No. 2016-20
April 2016

Seminar für Angewandte Mathematik
Eidgenössische Technische Hochschule
CH-8092 Zürich
Switzerland

PLASMONIC INTERACTION BETWEEN NANOSPHERES

SANGHYEON YU AND HABIB AMMARI

ABSTRACT. When metallic nanospheres are nearly touching, strong nanofocusing of light can occur due to highly localized surface plasmons. It has potential applications in the design of nanophotonic integrated circuits, biosensing, and spectroscopy. Due to the singular behavior of electromagnetic field in the narrow gap region, its analytical investigation is quite challenging. Moreover, it requires extremely large numerical cost for computing the field accurately. There are two approaches for studying the interaction between metallic spheres: transformation optics and the method of image charges. Here we clarify the connection between them. Based on the connection formula, we reveal the singular nature of plasmonic interaction between nanospheres in a completely analytical way. We also develop a hybrid numerical scheme for accurately and efficiently computing the field distribution produced by an arbitrary number of nearly touching plasmonic spheres.

1. INTRODUCTION

Confining light at the nanoscale is challenging due to the diffraction limit. Strongly localized surface plasmon modes in singular metallic structures offer a promising route to overcome this difficulty. Among various singular structures, the system of nearly touching spheres is of fundamental importance. In the narrow gap regions between metallic spheres, a broadband nanofocusing of light can be observed. Recently, Transformation Optics (TO) has been applied to analyze this phenomenon theoretically. Pendry et al. applied a TO inversion mapping to transform two spheres into a concentric shell and then provided novel physical insights for broadband light focusing. TO also gives a quasi-analytical solution which is an efficient numerical scheme. However, for a deeper theoretical understanding and practical purposes, fully analytical description is still needed. Roughly speaking, the difficulty comes from the inhomogeneous material parameters in the transformed space.

Beside analytical obstacles, there are also numerical challenges. When the spheres are nearly touching, it requires extremely large computational cost to accurately compute singular field distributions. The multipole expansion method requires a large number of moments and finite element method (or boundary element method) requires very fine mesh in the gap. Although the TO approach is efficient, it cannot be applied when the number of spheres is greater than two. It is important to investigate a cluster of plasmonic nanospheres for the design of fano-resonances.

In this article, we solve all these analytical and numerical challenges related to the singular nature of nearly touching plasmonic spheres. The key in our approach is to clarify the connection between TO and the method of image charges. The principle of image method is to find fictitious sources which generate the desired reaction field. We derive a new explicit formula to convert image sources to TO-type solutions. Our second key ingredient is the image theory developed by Poladian, who derived the image series solution for two dielectric spheres [23]. Nevertheless, the series is not convergent when the permittivity is negative and hence it cannot describe the plasmonic interaction. So our approach is to use the connection formula to convert the image series into a TO-type solution, resulting in a fully analytical approximate solution which is valid for two plasmonic spheres. Our formula is highly accurate for a broad range of frequencies and gap distances. Moreover, it gives clear understanding of the surface plasmon resonance.

For a cluster with an arbitrary number of spheres, Cheng and Greengard developed a hybrid numerical scheme by combining the method of images and the multipole expansion method. Their

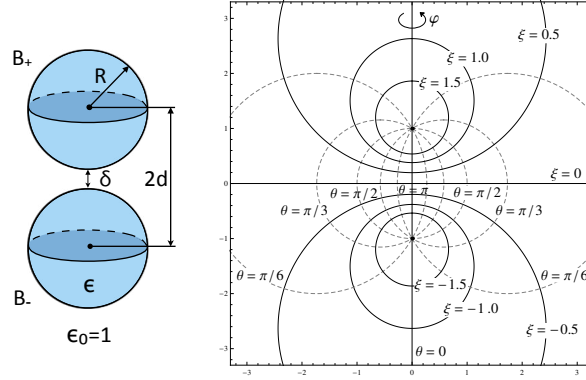


FIGURE 1. **Two spheres and the bispherical coordinates.** **Left:** Configuration of two spheres. $2d$ is the distance between the centers. δ is the gap distance. **Right:** coordinate level curves for the bispherical coordinate system with $\alpha = 1$. The solid line (resp. the dashed line) represents ξ (resp. η) coordinate curves.

scheme is extremely efficient and accurate even if the spheres are nearly touching. However, due to the non-convergence of the image series, their scheme needs to be modified for plasmonic spheres clusters. Again, by using the connection between TO and image sources, we develop the modified hybrid scheme for an arbitrary configuration of plasmonic spheres clusters. We also show its extreme efficiency and accuracy by presenting several numerical examples. Our proposed scheme is a result of beautiful interplay between three analytical approaches: TO, the image method, and the multipole expansion.

2. TRANSFORMATION OPTICS AND THE IMAGE METHOD

We shall assume that the plasmonic spheres are small compared to optical wavelengths so that the quasi-static approximation can be adopted. Two spheres system is described in Fig. 1. The permittivity ϵ of metallic spheres is modeled as $\epsilon = 1 - \omega_p^2/(\omega(\omega + i\gamma))$ where ω is the operating frequency, ω_p is the plasma frequency and γ is the damping parameter. We fit Palik's data for silver by adding a few Lorentz terms [18].

2.1. TO approach. Let us briefly review the TO approach by Pendry et al. [19]. To transform two spheres into a concentric shell, Pendry et al. introduced the inversion transformation Φ as

$$\mathbf{r}' = \Phi(\mathbf{r}) = R_T^2(\mathbf{r} - \mathbf{R}_0)/|\mathbf{r} - \mathbf{R}_0|^2 + \mathbf{R}'_0, \quad (1)$$

where $\mathbf{R}_0, \mathbf{R}'_0$ and R_T are given parameters. This inversion mapping induces the inhomogeneous permittivity $\epsilon'(\mathbf{r}') = R_T^2|\mathbf{r}' - \mathbf{R}'_0|\epsilon$ in the transformed space. Then, by taking advantage of the symmetry of the shell, they represented the electric potential using $|\mathbf{r}' - \mathbf{R}'_0|(r')^{\pm(n+\frac{1}{2})-\frac{1}{2}}Y_n^m(\theta', \phi')$ as basis functions. Here, $\{Y_n^m\}$ are the spherical harmonics.

The above TO description can be rewritten using the bispherical coordinates, (ξ, θ, φ) , as

$$e^{\xi - i\eta} = (z + i\rho + \alpha)/(z + i\rho - \alpha) \quad (2)$$

with $\rho = \sqrt{x^2 + y^2}$ and φ being an azimuthal angle with respect to the z -axis. By letting $\mathbf{r}' = e^\xi(\sin \eta \cos \varphi, \sin \eta \sin \varphi, \cos \eta)$, $\mathbf{R}'_0 = (0, 0, 1)$, $\mathbf{R}_0 = (0, 0, \alpha)$ and $R_T^2 = 2\alpha$, we can see that the bispherical transformation is identical to the inversion mapping in the TO approach. In Fig. 1, the geometry of the bispherical coordinates is described.

Any solution to the Laplace's equation can be represented as a sum of the following bispherical harmonics $\mathcal{M}_{n,\pm}^m(\mathbf{r})$:

$$\mathcal{M}_{n,\pm}^m(\mathbf{r}) = \sqrt{2}\sqrt{\cosh \xi - \cos \eta} e^{\pm(n+\frac{1}{2})\xi} Y_n^m(\eta, \varphi), \quad (3)$$

We will call $\mathcal{M}_{n,\pm}^m$ as TO basis since they are the same.

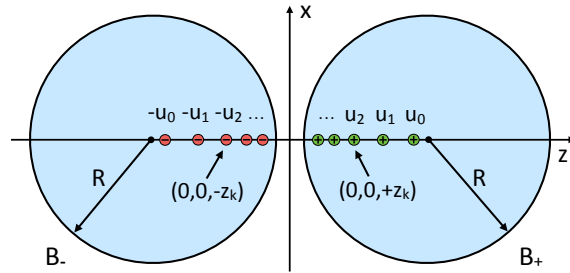


FIGURE 2. **Image charges for two spheres.** Red and green circles represent image charges placed along the z -axis.

Let us assume that two plasmonic spheres $B_+ \cup B_-$ are placed in a uniform incident field $(0, 0, E_0 \text{Re}\{e^{i\omega t}\})$. Then the quasi-static electric potential V outside the two spheres can be represented in the following form:

$$V(\mathbf{r}) = -E_0 z + \sum_{n=0}^{\infty} A_n (\mathcal{M}_{n,+}^0(\mathbf{r}) - \mathcal{M}_{n,-}^0(\mathbf{r})). \quad (4)$$

Here, the coefficients A_n satisfy some recurrence relations. We refer to [7] for details. The TO approach also yields a similar tridiagonal system for coefficients A_n [19]. Unfortunately, both of them cannot be solved analytically. The first goal in this work is to derive an approximate analytical expression for A_n by establishing the explicit connection between the method of images and TO.

2.2. Method of images. Now we discuss the method of images. Poladian developed a general framework of image sources for two dielectric spheres [22, 23, 24]. He also performed an asymptotic analysis for the nearly touching case. See also [13] for a similar result in the two-dimensional case. Here, we briefly review Poladian's solution for the two dielectric spheres in an uniform incident field. Let $\tau = (\epsilon - 1)/(\epsilon + 1)$, $s = \cosh^{-1}(d/R)$ and $\alpha = R \sinh s$. Suppose that two point charges of strength ± 1 are at $(0, 0, \pm z_0) \in B_{\pm}$, respectively. By Poladian's imaging rule, they produce an infinite series of image charges of strength $\pm u_k$ at $(0, 0, \pm z_k)$ for $k = 0, 1, 2, \dots$, where z_k and u_k are given by

$$z_k = \alpha \coth(ks + s + t_0), \quad u_k = \tau^k \frac{\sinh(s + t_0)}{\sinh(ks + s + t_0)}.$$

Here, the parameter t_0 is such that $z_0 = \alpha \coth(s + t_0)$. See Fig. 2. The potential $U(\mathbf{r})$ generated by all the above image charges is given by

$$U(\mathbf{r}) = \sum_{k=0}^{\infty} u_k (G(\mathbf{r} - \mathbf{z}_k) - G(\mathbf{r} + \mathbf{z}_k)), \quad (5)$$

where $\mathbf{z}_k = (0, 0, z_k)$ and $G(\mathbf{r}) = 1/(4\pi|\mathbf{r}|)$.

Let us consider the potential V outside the two spheres when a uniform incident field $(0, 0, E_0 \text{Re}\{e^{i\omega t}\})$ is applied. Let p_0 be the induced polarizability when a single sphere is subjected to the uniform incident field, that is, $p_0 = E_0 R^3 2\tau/(3 - \tau)$. Using the potential $U(\mathbf{r})$, we can derive an approximate solution for $V(\mathbf{r})$. For $|\tau| \approx 1$, we have

$$V(\mathbf{r}) \approx -E_0 z + 4\pi p_0 \left. \frac{\partial(U(\mathbf{r}))}{\partial z_0} \right|_{z_0=d} + QU(\mathbf{r})|_{z_0=d}, \quad (6)$$

where Q is a constant chosen so that the right-hand side in equation (6) has no net flux on the surface of each sphere; see SI for the details. The accuracy of the approximate formula, equation

(6), improves as $|\epsilon|$ increases and it becomes exact when $|\epsilon| = \infty$. Moreover, the accuracy of equation (6) is pretty good even if the value of $|\epsilon|$ is moderate.

Now we discuss the difficulty in applying the approximate formula (6) to the case of plasmonic spheres. In view of the expressions for u_k , we can see that equation (6) is not convergent when $|\tau| > e^s$. For plasmonic materials such as gold and silver, the real part of the permittivity ϵ is negative over the optical frequencies and then the corresponding parameter $|\tau|$ can attain any value in the interval (e^s, ∞) . Moreover, it turns out that all the plasmonic resonant values for τ are contained in the set $\{\tau \in \mathbb{C} : |\tau| > e^s\}$. So, equation (6) cannot be applied to describe the plasmonic interaction between spheres due to non-convergence.

3. ANALYTICAL SOLUTION FOR THE TWO PLASMONIC SPHERES

So far we have reviewed TO approach and the image method and pointed out their difficulties in solving the two plasmonic spheres problem. Now we clarify the connection between these two methods and then derive the approximate analytical solution for the scattered field from two plasmonic spheres. We also show that our analytical expression completely captures the singular behavior of the exact solution.

3.1. Connection formula from image charges to TO. We derive for the first time an explicit formula connecting the image charges and TO. We state the following lemma (see SI for its proof).

Lemma 1. (Connection formula) *The potential $u_k G(\mathbf{r} \mp \mathbf{z}_k)$ generated by the image charge at $\pm \mathbf{z}_k$ can be rewritten using TO basis as follows: for $\mathbf{r} \in \mathbb{R}^3 \setminus (B_+ \cup B_-)$, we have*

$$u_k G(\mathbf{r} \mp \mathbf{z}_k) = \frac{\sinh(s + t_0)}{4\pi\alpha} \sum_{n=0}^{\infty} [\tau e^{-(2n+1)s}]^k e^{-(2n+1)(s+t_0)} \mathcal{M}_{n,\pm}^0(\mathbf{r}). \quad (7)$$

This identity plays a key role in our derivation of the approximate analytical solution. As mentioned previously, the reason why the image charge series, equation (5), does not work for plasmonic spheres is because the factor $(\tau e^{-s})^k$ may not converge to zero as $k \rightarrow \infty$. But the above connection formula helps us overcome this difficulty. If we sum up all the image charges in equation (7), we can see that the summation over k can be evaluated analytically using the following identity:

$$\sum_{k=0}^{\infty} [\tau e^{-(2n+1)s}]^k = \frac{e^{(2n+1)s}}{e^{(2n+1)s} - \tau}. \quad (8)$$

Therefore, from equation (5) and Lemma 1, we obtain the following result.

Theorem 2. *Let $U(\mathbf{r})$ be defined as in equation (5). Then it can be rewritten using TO basis as follows:*

$$U(\mathbf{r}) = \frac{\sinh(s + t_0)}{4\pi\alpha} \sum_{n=0}^{\infty} \frac{e^{-(2n+1)t_0}}{e^{(2n+1)s} - \tau} \left(\mathcal{M}_{n,+}^0(\mathbf{r}) - \mathcal{M}_{n,-}^0(\mathbf{r}) \right). \quad (9)$$

Clearly, the right-hand side of equation (9) does converge for any $|\tau| > e^s$ provided that $\tau \neq e^{(2n+1)s}$.

3.2. Approximate analytical solution. Let us turn to the problem of two plasmonic spheres in an uniform incident field $(0, 0, E_0 \text{Re}\{e^{i\omega t}\})$. From equation (6) and Theorem 2, we obtain the approximate expression for $V(\mathbf{r})$ in terms of TO basis as follows (see SI for its proof).

Theorem 3. *If $|\tau| \approx 1$, the following approximation for the electric potential $V(\mathbf{r})$ holds: for $\mathbf{r} \in \mathbb{R}^3 \setminus (B_+ \cup B_-)$,*

$$V(\mathbf{r}) \approx -E_0 z + \sum_{n=0}^{\infty} \tilde{A}_n \left(\mathcal{M}_{n,+}^0(\mathbf{r}) - \mathcal{M}_{n,-}^0(\mathbf{r}) \right), \quad (10)$$

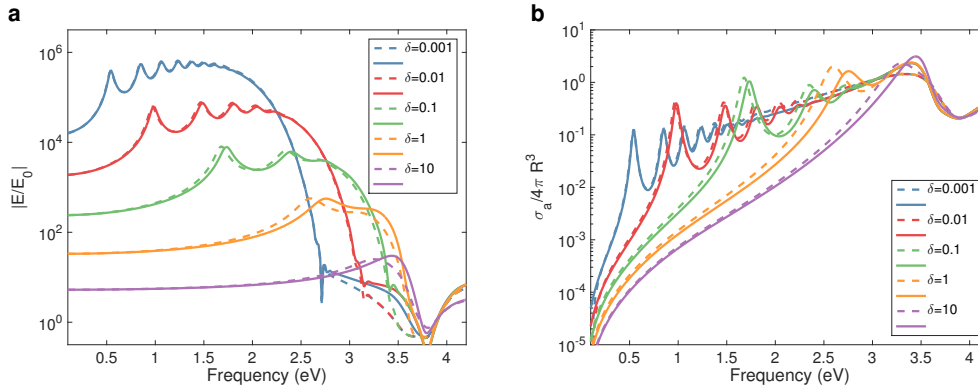


FIGURE 3. **Field and absorption cross section enhancement.** $R = 30$ nm. Solid line represents the approximate analytical solution. Dashed line represents the exact solution. (a): field enhancement (b): absorption cross section.

where the coefficient \tilde{A}_n is given by

$$\tilde{A}_n = E_0 \frac{2\tau\alpha}{3-\tau} \cdot \frac{2n+1-\gamma_0}{e^{(2n+1)s}-\tau}, \quad (11)$$

$$\gamma_0 = \sum_{n=0}^{\infty} \frac{2n+1}{e^{(2n+1)s}-\tau} \bigg/ \sum_{n=0}^{\infty} \frac{1}{e^{(2n+1)s}-\tau}. \quad (12)$$

As expected, the above approximate expression is valid even if $|\tau| > e^s$. Therefore, it can furnish useful information about the plasmonic interaction between the two spheres. As a first demonstration, let us investigate the (approximate) resonance condition for the bright modes, that is, the condition for τ at which the coefficients \tilde{A}_n diverge. One might conclude that the resonance condition is given by $\tau = e^{(2n+1)s}$. However, one can see that \tilde{A}_n has a removable singularity at each $\tau = e^{(2n+1)s}$. In fact, the (approximate) resonance condition turns out to be

$$\sum_{n=0}^{\infty} \frac{1}{e^{(2n+1)s}-\tau} = 0. \quad (13)$$

In other words, the plasmonic resonance does happen when τ is one of zeros of equation (13). It turns out that the zeros $\{\tau_n\}_{n=0}^{\infty}$ lie on the positive real axis and satisfy, for $n = 0, 1, 2, \dots$,

$$e^{(2n+1)s} < \tau_n < e^{(2n+3)s}. \quad (14)$$

Now let us discuss the asymptotic behavior of the resonance when two spheres are nearly touching. As the separation distance δ goes to zero, the parameter s also goes to zero (in fact, $s = O(\delta^{1/2})$). Then, in view of equation (14), τ_n will converge to 1 and the corresponding permittivity ϵ_n goes to infinity. This means that a red-shift of the resonance mode does occur. Since the approximate analytical formula for V becomes more accurate as $|\epsilon|$ increases, we can expect that accuracy improves as the separation distance goes to zero. It indicates that the formula contains singular nature of the field distribution completely. Also, the difference between τ_n and τ_{n+1} decreases, which means that the spectrum becomes a nearly continuous one.

It is worth mentioning that the resonance condition, equation (13), is also interesting from a mathematical point of view. It is known that the plasmon resonance occurs when $1/(2\tau)$ is close to one of the eigenvalues of the Neumann-Poincaré operator [2]. So equation (13) gives the approximate eigenvalues of the Neumann-Poincaré operator in the case of two spheres.

3.3. Field and absorption cross section enhancements. Here, we derive approximate formulas for the field at the gap and for the absorption cross section. From Theorem 3, we derive the

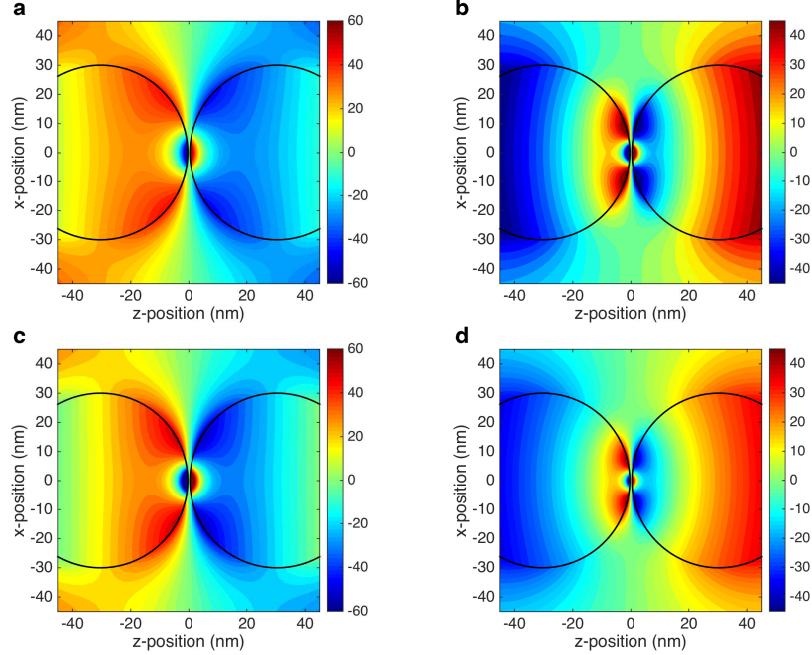


FIGURE 4. **Potential distributions.** $R = 30$ nm, $\delta = 0.25$ nm, $\omega = 3.0$ eV, **(a,b)**: Real and imaginary parts of the exact solution. **(c,d)**: Real and imaginary parts of the analytical approximate solution.

following (see SI for the details):

$$E(0, 0, 0) \approx E_0 - E_0 \frac{8\tau}{3 - \tau} \left[\sum_{n=0}^{\infty} \frac{(2n+1)^2}{e^{(2n+1)s} - \tau} (-1)^n - \gamma_0 \sum_{n=0}^{\infty} \frac{2n+1}{e^{(2n+1)s} - \tau} (-1)^n \right]. \quad (15)$$

In the quasi-static approximation, the absorption cross section σ_a is defined by $\sigma_a = \omega \text{Im}\{p\}$, where p is the polarizability of the system of two spheres and ω is the operating frequency. From Theorem 3, σ_a is approximated as follows (see again SI):

$$\sigma_a \approx \omega E_0 \frac{8\tau\alpha^3}{3 - \tau} \left[\sum_{n=0}^{\infty} \frac{(2n+1)^2}{e^{(2n+1)s} - \tau} - \left(\sum_{n=0}^{\infty} \frac{2n+1}{e^{(2n+1)s} - \tau} \right)^2 / \sum_{n=0}^{\infty} \frac{1}{e^{(2n+1)s} - \tau} \right]. \quad (16)$$

Now we compare the above approximate formulas with the exact ones. Fig. 3 represents respectively the field enhancement and the absorption cross section σ_a as functions of the frequency ω for various distances ranging from 0.001 nm to 10 nm. The good accuracy of our approximate formulas over broad ranges of frequencies and the gap distances is clearly shown. As mentioned previously, the accuracy improves as the spheres get closer. It is also worth highlighting the red-shift of the plasmon resonance as the separating distance goes to zero. In Fig. 4, we compare exact and approximate electric potential distributions. They are also in good agreement and the field concentration in the gap region is observed.

4. HYBRID NUMERICAL SCHEME FOR MANY-SPHERES SYSTEM

Now we consider a system of an arbitrary number of plasmonic spheres. If all the spheres are well separated, then the multipole expansion method is efficient and accurate for computing the field distribution (see SI). But, when the spheres are close to each other, the problem becomes very challenging since the charge densities on each sphere are nearly singular. To overcome this difficulty, in [5], Cheng and Greengard developed a hybrid numerical scheme combining the multipole expansion and the method of images; see also [6]. Their algorithm is extremely efficient and highly accurate even if the distance between the spheres is extremely small. However, due to non-convergence of the image series, their method cannot be applied to plasmonic spheres. The second goal of this paper is to show that the hybrid method can be extended to the system of plasmonic spheres by clarifying the connection between the method of images and TO.

The key ingredient in the hybrid method by Cheng and Greengard is the image source series produced by a general multipole source. Roughly speaking, Cheng and Greengard modified the multipole expansion method by replacing a multipole source with the image multipole potential. Let $\mathcal{Y}_{lm}(\mathbf{r})$ be a general multipole source, that is, $\mathcal{Y}_{lm}(\mathbf{r}) = Y_l^m(\theta, \phi)/r^{l+1}$. Suppose that a multipole source \mathcal{Y}_{lm} is located at the center of the sphere B_+ . Then the infinite sequence of the image sources is produced by Poladian's imaging rule. Let us denote the resulting potential by U_{lm}^+ . Similarly, let U_{lm}^- be the corresponding potential when the initial position is the center of B_- . The detailed image series representation for U_{lm}^\pm can be found in SI. Again, the series are not convergent for $|\tau| > e^s$. Therefore, for extending Cheng and Greengard's method to the plasmonic case, it is essential to establish an explicit connection between the image multipole potential U_{lm}^\pm and TO. We have the following result whose proof is given in SI.

Theorem 4. (*Converting image multipoles to TO*) Assume that the integers l and m are such that $l \geq 1$ and $-l \leq m \leq l$. The potential U_{lm}^\pm can be rewritten in terms of TO basis as follows: for $\mathbf{r} \in \mathbb{R}^3 \setminus (B_+ \cup B_-)$,

$$\begin{aligned} U_{lm}^\pm(\mathbf{r}) &= \sum_{n=0}^{\infty} \frac{g_n^m \mathcal{D}_{lm}^\pm[\lambda_n^m]}{e^{2(2n+1)s} - \tau^2} (e^{(2n+1)s} \mathcal{M}_{n,\pm}^m(\mathbf{r}) - \tau \mathcal{M}_{n,\mp}^m(\mathbf{r})) \\ &\quad - \delta_{0m} \frac{\tilde{Q}_{l,1}^\pm}{2} \sum_{n=0}^{\infty} \frac{\mathcal{M}_{n,+}^0(\mathbf{r}) + (-1)^l \mathcal{M}_{n,-}^0(\mathbf{r})}{e^{(2n+1)s} + (-1)^l \tau} \\ &\quad \mp \delta_{0m} \frac{\tilde{Q}_{l,2}^\pm}{2} \sum_{n=0}^{\infty} \frac{\mathcal{M}_{n,+}^0(\mathbf{r}) - (-1)^l \mathcal{M}_{n,-}^0(\mathbf{r})}{e^{(2n+1)s} - (-1)^l \tau}, \end{aligned} \quad (17)$$

where $g_n^m, \lambda_n^m, \mathcal{D}_{lm}^\pm$ and Q_l^\pm are given by

$$g_n^m = \frac{1}{\alpha^{|m|+1}} \frac{2^{|m|}}{\sqrt{(2|m|)!}} \sqrt{\frac{(n+|m|)!}{(n-|m|)!}}, \quad (18)$$

$$\lambda_n^m = [\sinh(s+t_0)]^{2|m|+1} e^{-(2n+1)t_0}, \quad (19)$$

$$N_{lm} = (l-|m|)! \sqrt{\binom{l+|m|}{l+m} \binom{l+|m|}{|m|+m}}, \quad (20)$$

$$\mathcal{D}_{lm}^\pm[f] = \frac{(\pm 1)^{l-|m|}}{N_{lm}} \frac{\partial^{l-|m|}}{\partial [z_0(t_0)]^{l-|m|}} f \Big|_{z_0=d}. \quad (21)$$

$$\tilde{Q}_{l,i}^\pm = \sum_{n=0}^{\infty} \frac{(\pm 1)^l g_n^0 \mathcal{D}_{l0}^\pm[\lambda_n^0]}{e^{(2n+1)s} - (-1)^{l+i} \tau} \Big/ \sum_{n=0}^{\infty} \frac{1}{e^{(2n+1)s} - (-1)^{l+i} \tau}. \quad (22)$$

Here, δ_{lm} is the Kronecker delta.

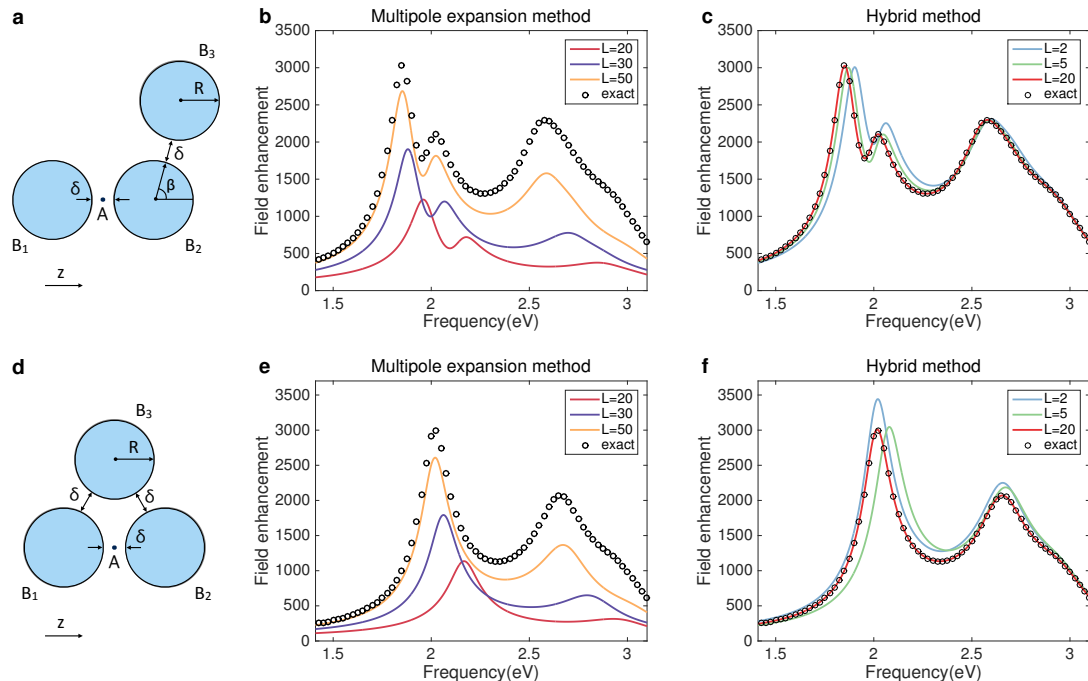


FIGURE 5. **Multipole expansion method vs Hybrid scheme.** (a,d): Two examples of three spheres configurations. (b,c): Plot for the field enhancement at point A for configuration (a) using the multipole expansion method and the hybrid method. $R = 30\text{nm}$, $\delta = 0.25\text{ nm}$, $\beta = 80^\circ$ (e,f): same but for configuration (d).

Clearly, the above TO representation for U_{lm}^\pm does converge for $|\tau| > e^s$. Based on this, we develop the modified hybrid scheme for the plasmonic spheres system. For a detailed description of the proposed numerical scheme, we refer to SI.

Next, we present numerical examples to illustrate the hybrid method. We consider two examples of the three-spheres configuration shown in Figs. 5a and 5d. We show comparison between multipole expansion method and the hybrid method by plotting the field enhancement at the gap center A. For the numerical implementation, only finite number of the multipoles \mathcal{Y}_{lm} or hybrid multipoles U_{lm}^\pm should be used. Let L be the truncation number for the order l . In Figs. 5b and 5e, the field enhancement is computed using the standard multipole expansion method. The computations give inaccurate results even if we include a large number of multipole sources with $L = 50$. On the contrary, using the hybrid method (Figs. 5c and 5f), the accuracy is pretty good even when L is small ($L = 2$ or $L = 5$). Also, 99% accuracy can be achieved only with $L = 20$. For each hybrid multipole U_{lm}^\pm , the TO harmonics are included upto order $n = 300$ to ensure convergence and U_{lm}^\pm can be evaluated very efficiently.

To achieve 99.9% accuracy at the first resonant peak, it is required to set $L = 150$ in the multipole expansion method and a $68,400 \times 68,400$ linear system needs to be solved. However, the same accuracy can be achieved only with $L = 23$ in the hybrid method. The corresponding linear system's size is $1,725 \times 1,725$ and it can be solved 2,000 times faster than that of the multipole expansion method. The reason for the extreme efficiency and accuracy is that the singular nature of the field distribution is already captured analytically in the hybrid multipole U_{lm}^\pm . We also compute the field distribution for three-spheres examples in Fig. 6. High field concentration in the narrow gap regions between nanospheres is clearly shown.

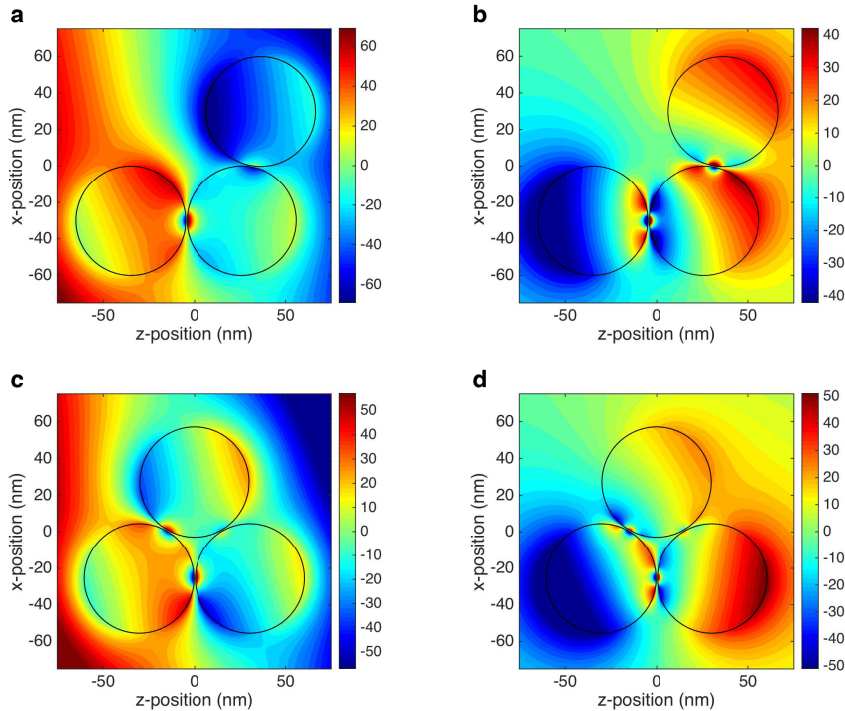


FIGURE 6. **Potential distribution for three spheres examples.** (a,b): Real and imaginary part of the potential for the configuration in Fig. 5a with $\beta = 80^\circ$. $R = 30$ nm, $\delta = 0.25$ nm, $\omega = 3.0$ eV. The uniform incident field $(E_0 \sin 15^\circ, 0, E_0 \cos 15^\circ) \text{Re}\{e^{i\omega t}\}$ is applied. (c,d): same but for the configuration in Fig. 5d.

5. DISCUSSION

In this article we have fully characterized the singular behavior of nearly touching plasmonic nanospheres in an analytical way. We have derived an approximate analytical formula for the electric field for two plasmonic spheres. The formula is highly accurate for wide ranges of complex permittivities (or frequencies) and gap distances. Finally, we have extended Cheng and Greengard's hybrid method to the case of plasmonic spheres. The extreme efficiency and accuracy is shown by several numerical examples. We have assumed that the spheres are identical only for simplicity. Our approach can be directly extended to the case where the spheres are not equisized and have different material parameters. A system of nanospheres on a plane (or a substrate) can also be considered. The nonlocal effect is an important issue when the spheres are extremely closely spaced. By adopting the shifting boundary method developed by Luo et al [12], this effect can be easily incorporated.

6. ACKNOWLEDGMENTS

The authors would like to thank R.C. McPhedran and G.W. Milton for pointing out the existence of Poladian's thesis [22].

REFERENCES

- [1] H. Ammari, Y. Deng, and P. Millien, Surface plasmon resonance of nanoparticles and applications in imaging, *Arch. Ration. Mech. Anal.*, 220 (2016), 109–153.
- [2] H. Ammari, M. Ruiz, S. Yu, and H. Zhang, Mathematical analysis of plasmonic resonances for nanoparticles: the full Maxwell equations, arXiv:1511.06817.

- [3] H. Ammari, G. Ciraolo, H. Kang, H. Lee, and K. Yun, Spectral analysis of the Neumann-Poincaré operator and characterization of the stress concentration in anti-plane elasticity. *Arch. Ration. Mech. Anal.* 208 (2013), 275–304.
- [4] E.S. Bao, Y.Y. Li, and B. Yin, Gradient estimates for the perfect conductivity problem, *Arch. Ration. Mech. Anal.* 193 (2009), 195–226.
- [5] H. Cheng and L. Greengard, A method of images for the evaluation of electrostatic fields in systems of closely spaced conducting cylinders, *SIAM J. Appl. Math.*, 58 (1998) 121–141.
- [6] H. Cheng, On the method of images for systems of closely spaced conducting spheres, *SIAM J. Appl. Math.*, 61 (2000) 1324–1337.
- [7] A. Goyette and A. Navon, Two dielectric spheres in an electric field, *Phys. Rev. B* 13 (1976) 4320–4327.
- [8] H. Kang, M. Lim, and K. Yun, Characterization of the electric field concentration between two adjacent spherical perfect conductors, *SIAM J. Appl. Math.*, 74 (2014), 125–146.
- [9] V.V. Lebedev, S.S. Vergeles, and P.E. Vorobev, Surface modes in metalinsulator composites with strong interaction of metal particles, *Appl. Phys. B*, 111 (2013), 577–588.
- [10] S. Link and M.A. El-Sayed, Spectral properties and relaxation dynamics of surface plasmon electronic oscillations in gold and silver nanodots and nanorods, *J. Phys. Chem. B*, 103 (1999), 8410–8426.
- [11] V. V. Klimov and D. V. Guzatov, Strongly localized plasmon oscillations in a cluster of two metallic nanospheres and their influence on spontaneous emission of an atom, *Phys. Rev. B*, 75 (2007) 024303.
- [12] Y. Luo, R. Zhao, and J.B. Pendry, van der Waals interactions at the nanoscale: The effects of nonlocality, *PNAS* 111 (2014), 18422–18427.
- [13] R. C. McPhedran, L. Poladian and G. W. Milton, Asymptotic studies of closely spaced, highly conducting cylinders, *Proc. Roy. Soc. A*, 415 (1988), 185–196.
- [14] P. Moon and D.E. Spencer, *Field Theory Handbook*, 2nd Ed. Springer-Verlag, Berlin, 1988.
- [15] C. Neumann, *Hydrodynamische Untersuchungen nebst einem Anhang über die Probleme der Electrostatik und der magnetischen Induktion*, Teubner, Leipzig, 1883, 279–282.
- [16] O. Schnitzer, Singular perturbations approach to localised surface-plasmon resonance: nearly touching metal nano-spheres, arXiv:1508.04947.
- [17] O. Schnitzer, V. Giannini, R.V. Craster, and S.A. Maier, Asymptotics of surface-plasmon redshift saturation at sub-nanometric separations, arXiv:1511.04895.
- [18] E.D. Palik, *Handbook of Optical Constants of Solids*, Academic Press, 1985.
- [19] J.B. Pendry, A. I. Fernández-Domínguez, Y. Luo, and R. Zhao, Capturing photons with transformation optics, *Nature Phys.*, 9 (2013), 518–522.
- [20] J.B. Pendry, Y. Luo, and R. Zhao, Transforming the optical landscape, *Science*, 348 (2015), 521–524.
- [21] J.B. Pendry, A. Aubry, D.R. Smith, and S.A. Maier, Transformation optics and subwavelength control of light, *Science*, 337 (2012), 549–552.
- [22] L. Poladian, *Effective Transport and Optical Properties of Composite Materials*, Ph.D. thesis, University of Sydney, 1990.
- [23] L. Poladian, General theory of electrical images in sphere pairs, *Q. J. Mech. Appl. Math.*, 41 (1988), 395–417.
- [24] L. Poladian, Asymptotic behaviour of the effective dielectric constants of composite materials, *Proc. Roy. Soc. A*, 426 (1988), 343–359.
- [25] I. Romero, J. Aizpurua, G.W. Bryant, and F. Javier García de Abajo, Plasmons in nearly touching metallic nanoparticles: singular response in the limit of touching dimers, *Opt. Expr.*, 14 (2006), 9988–9999.
- [26] W.R. Smythe, *Static and Dynamic Electricity*, McGraw-Hill, New York, 1950.

DEPARTMENT OF MATHEMATICS, ETH ZÜRICH, RÄMISTRASSE 101, CH-8092 ZÜRICH, SWITZERLAND
E-mail address: sanghyeon.yu@math.ethz.ch

DEPARTMENT OF MATHEMATICS, ETH ZÜRICH, RÄMISTRASSE 101, CH-8092 ZÜRICH, SWITZERLAND
E-mail address: habib.ammari@math.ethz.ch

SUPPLEMENTARY MATERIAL FOR "PLASMONIC INTERACTION BETWEEN NANOSPHERES"

SANGHYEON YU AND HABIB AMMARI

The supplementary material (SI) is organized as follows. In section 1, we review the basics of the bispherical coordinates. In section 2, we collect various definitions and some of the properties of spherical harmonics. In section 3, we review Poladian's method of images for two spheres. In section 4, we prove our main result, which provides the connection between the Transformation Optics (TO) and the method of images. In section 5, we discuss the hybrid numerical scheme for the system of plasmonics spheres. In section 6, we prove various useful formulas. For clarity and convenience, some parts of SI overlap with the main text.

1. BISPHERICAL COORDINATES (INVERSION MAPPING IN TO)

Here we review the definition and the properties of the bispherical coordinates. The bispherical coordinate system, (ξ, θ, φ) , is defined by

$$e^{\xi - i\theta} = (z + i\rho + \alpha)/(z + i\rho - \alpha), \quad (1)$$

where $\rho = \sqrt{x^2 + y^2}$ and α is a positive constant. The Cartesian coordinates can be written in terms of the bispherical ones as follows:

$$x = \frac{\alpha \sin \eta \cos \varphi}{\cosh \xi - \cos \eta}, \quad y = \frac{\alpha \sin \eta \sin \varphi}{\cosh \xi - \cos \eta}, \quad z = \frac{\alpha \sinh \xi}{\cosh \xi - \cos \eta}. \quad (2)$$

Note that the origin $(0, 0, 0)$ corresponds to $\xi = 0, \eta = \pi, \varphi = 0$. The point at infinity corresponds to $(\xi, \eta) \rightarrow (0, 0)$. On the other hand, it can be easily shown that the coordinate surfaces $\{\xi = c\}$ and $\{\theta = c\}$ for a nonzero c are respectively the zero level set of

$$f^\xi(x, y, z) = (z - \alpha \coth c)^2 + \rho^2 - (\alpha/\sinh c)^2, \quad (3)$$

$$f^\eta(x, y, z) = (\rho - \alpha \cot c)^2 + z^2 - (\alpha/\sin c)^2. \quad (4)$$

Note also that the ξ -coordinate surface is the sphere of radius $\alpha/\sinh c$ centered at $(0, 0, \alpha \coth c)$. Therefore, $\xi = c$ (or $\xi = -c$) represents a sphere contained in the region $z > 0$ (resp. $z < 0$). Moreover, $|\xi| < c$ (resp. $|\xi| > c$) represents the region outside (resp. inside) the two spheres.

Suppose that two spheres B_+ and B_- of the same radius R are centered at $(0, 0, +d)$ and $(0, 0, -d)$, respectively. Let us parameterize these two spheres by $\{\xi = \pm s\}$. To do this, we set s and α by $d = \alpha \coth s$ and $R = \alpha \sinh s$ in view of (3). Note that $d = (\alpha/\sinh s) \cosh s = R \cosh s$.

It is well-known that any solution to the Laplace equation can be represented as a sum of the following bispherical harmonics $\mathcal{M}_{n,\pm}^m(\mathbf{r})$:

$$\mathcal{M}_{n,\pm}^m(\mathbf{r}) = \sqrt{2} \sqrt{\cosh \xi - \cos \eta} e^{\pm(n+\frac{1}{2})\xi} Y_n^m(\eta, \varphi).$$

The scale factors for the bispherical coordinates are

$$\sigma_\xi = \sigma_\eta = \frac{\alpha}{\cosh \xi - \cos \eta} \quad \text{and} \quad \sigma_\varphi = \frac{\alpha \sin \eta}{\cosh \xi - \cos \eta},$$

so that the gradient for scalar valued function g can be written in the form

$$\nabla g = \frac{1}{\sigma_\xi} \frac{\partial g}{\partial \xi} \hat{\mathbf{e}}_\xi + \frac{1}{\sigma_\eta} \frac{\partial g}{\partial \eta} \hat{\mathbf{e}}_\eta + \frac{1}{\sigma_\varphi} \frac{\partial g}{\partial \varphi} \hat{\mathbf{e}}_\varphi.$$

The normal derivative on the sphere $\{\xi = \pm s\}$ is given by

$$\left. \frac{\partial}{\partial \mathbf{n}} \right|_{\partial B_\pm} = \mp \hat{\mathbf{e}}_\xi \cdot \nabla \Big|_{\partial B_\pm} = \mp \frac{\cosh s - \cos \eta}{\alpha} \left. \frac{\partial}{\partial \xi} \right|_{\xi = \pm s}, \quad (5)$$

where \mathbf{n} denotes the outward unit normal vector.

If the function g is of the following form:

$$g(\mathbf{r}) = \sum_{n=0}^{\infty} \sum_{m=-n}^n c_n^m \mathcal{M}_{n,+}^m(\mathbf{r}) + d_n^m \mathcal{M}_{n,-}^0(\mathbf{r}),$$

then z -component of the gradient at the origin is given by

$$\hat{\mathbf{e}}_z \cdot \nabla g(0, 0, 0) = \frac{2^{3/2}}{\alpha} \sum_{n=0}^{\infty} (c_n^0 - d_n^0) (n+1/2) (-1)^n, \quad (6)$$

where $\hat{\mathbf{e}}_z = (0, 0, 1)$.

2. SOME DEFINITIONS AND PROPERTIES

- Let us define the spherical harmonics Y_l^m by

$$Y_{lm}(\theta, \phi) = \sqrt{\frac{(l-|m|)!}{(l+|m|)!}} P_l^{|m|}(\cos \theta) e^{im\phi},$$

where $P_l^m(x)$ is the associated Legendre polynomial given by

$$P_l^m(x) = (-1)^m (1-x^2)^{m/2} \frac{d^m}{dx^m} P_l(x).$$

Here, $P_l(x)$ is the Legendre polynomial of degree l .

- The Legendre polynomial $P_n(x)$ has the following generating function:

$$\frac{1}{\sqrt{1-2xt+t^2}} = \sum_{n=0}^{\infty} t^n P_n(x). \quad (7)$$

- The associated Legendre polynomial $P_n^m(x)$ has the following generating function:

$$(-1)^m (2m-1)!! \frac{(1-x^2)^{m/2} t^m}{[1-2xt+t^2]^{m+1/2}} = \sum_{n=0}^{\infty} t^n P_n^m(x). \quad (8)$$

- We have

$$P_n^n(x) = (-1)^n (2n-1)!! (1-x^2)^{n/2}. \quad (9)$$

- Let us define the solid harmonics \mathcal{Y}_{lm} and \mathcal{Z}_{lm} by

$$\begin{aligned} \mathcal{Y}_{lm}(\mathbf{r}) &= r^{-(l+1)} Y_{lm}(\theta, \phi), \\ \mathcal{Z}_{lm}(\mathbf{r}) &= r^l Y_{lm}(\theta, \phi). \end{aligned}$$

- Let us introduce

$$w_{lm} = \begin{cases} 1, & m \geq 0, \\ (-1)^{|m|}, & m < 0. \end{cases}$$

- Let the constant N_{lmab} be given by

$$N_{lmab} = (-1)^{a+b} \sqrt{\binom{l+a-b+m}{l+m} \binom{l+a+b-m}{a+b}}.$$

3. POALDIAN'S IMAGE SOLUTION FOR TWO SPHERES (REVIEW)

3.1. Two spheres in an uniform electric field. Here, we briefly review Poladian's solution for the two dielectric spheres. Let $G(\mathbf{r}) = 1/(4\pi|\mathbf{r}|)$ be the electric potential generated by a unit point charge. We also introduce the electric potential $D(\mathbf{r}) = \mathbf{e}_z \cdot \hat{\mathbf{r}}/(|\mathbf{r}|^2)$ generated by a point dipole source with unit moment \mathbf{e}_z , where $\hat{\mathbf{r}} = \mathbf{r}/|\mathbf{r}|$.

Suppose that we locate a point charge of the magnitude ± 1 at the position $(0, 0, \pm z_0)$ in the sphere B_{\pm} , respectively. These point charges induce infinite series of image charges. Let us denote the location of m -th image charge in the sphere B_{\pm} by $\pm \mathbf{z}_m = (0, 0, \pm z_m)$, respectively. We also let $\pm u_m$ to be the magnitude of m -th image charge in the sphere B_{\pm} , respectively. Using Poladian's imaging rule, we can easily see that z_m and u_m satisfy the following recursive relations:

$$d - z_{k+1} = \frac{R^2}{d + z_k}, \quad u_{k+1} = \tau \frac{R}{d + z_k} u_k.$$

These recursive relations can be solved explicitly. To state the solutions for u_k and z_k , we introduce a parameter t_0 which satisfies

$$z_0 = \alpha \coth(s + t_0).$$

Note that if the initial position is equal to the center of each sphere (that is, $z_0 = d = R \cosh s$), then it holds that $t_0 = 0$. Using this representation for z_0 and the hyper-trigonometric identities, one can see that the solutions for z_k and u_k are given as follows:

$$\begin{aligned} z_k &= \alpha \coth(ks + s + t_0), \\ u_k &= \tau^k \frac{\sinh(s + t_0)}{\sinh(ks + s + t_0)}. \end{aligned}$$

Now the potential $U(\mathbf{r})$ generated by all the above image charges is given by

$$U(\mathbf{r}) = \sum_{k=0}^{\infty} u_k (G(\mathbf{r} - \mathbf{z}_k) - G(\mathbf{r} + \mathbf{z}_k)), \quad (10)$$

where $\mathbf{z}_k = (0, 0, z_k)$.

Let us now turn to original problem: two spheres in a uniform electric field $(0, 0, E_0)$. Let $\tau = (\epsilon - 1)/(\epsilon + 1)$ and let p_0 be the induced polarizability when a single sphere is probed by a uniform electric field E_0 , that is, $p_0 = E_0 R^3 2\tau/(3 - \tau)$. When two spheres are probed by a uniform electric field, the external field is first imaged in each sphere. An image dipole with moment p_0 is induced at the center of each sphere. Then these images are imaged back and forth between the spheres producing an infinite sequence of images [4]. The dipole p_0 can be considered as the limit of two initial charges $\pm 4\pi p_0/2h$ at the points $z_0 = (0, 0, d \pm h)$ as $h \rightarrow 0$. It is equivalent to taking derivative $4\pi p_0 \partial/\partial z_0$ at $z_0 = d$. So we get the following expression for the image potential generated by the point dipole p_0 :

$$V_1(\mathbf{r}) := 4\pi p_0 \frac{\partial(U(\mathbf{r}))}{\partial z_0} \Big|_{z_0=d}. \quad (11)$$

Since we have

$$\frac{\partial}{\partial z_0} \Big|_{z_0=d} = -\frac{\sinh^2 s}{\alpha} \frac{\partial}{\partial t_0} \Big|_{t_0=0}, \quad (12)$$

we can represent V_1 more explicitly in the form

$$V_1(\mathbf{r}) = \sum_{m=0}^{\infty} p_m D(\mathbf{r} - \mathbf{r}_m) - q_m G(\mathbf{r} - \mathbf{r}_m) \\ + \sum_{m=0}^{\infty} p_m D(\mathbf{r} + \mathbf{r}_m) + q_m G(\mathbf{r} + \mathbf{r}_m),$$

where \mathbf{r}_m , p_m and q_m are given by

$$\mathbf{r}_m = \mathbf{z}_m|_{t_0=0} = (0, 0, \alpha \coth(m+1)s), \\ p_m = \tau^m p_0 \left(\frac{\sinh s}{\sinh(m+1)s} \right)^3, \quad q_m = \tau^m \frac{p_0 \sinh s \sinh ms}{R \sinh^2(m+1)s}.$$

As pointed out by Poladian in [4], the potential V_1 is unphysical because the total charge on each sphere is non-zero. We have to neutralize them. Following Poladian's strategy, we introduce an additional potential by locating a point charge $\pm Q$ at the center of the sphere B_{\pm} , respectively. Then the corresponding image potential is

$$V_2(\mathbf{r}) := QU(\mathbf{r})|_{z_0=d} \\ = Q \sum_{m=0}^{\infty} u_m^0 (G(\mathbf{r} - \mathbf{r}_m) - G(\mathbf{r} + \mathbf{r}_m)),$$

where u_k^0 is defined by

$$u_k^0 = u_k|_{t_0=0} = \tau^k \frac{\sinh s}{\sinh(k+1)s}.$$

Now we choose the constant Q so that the potential $V_1 + V_2$ has no net flux on each sphere. Then Q becomes

$$Q = \sum_{j=0}^{\infty} q_j / \sum_{j=0}^{\infty} u_m^0. \quad (13)$$

Finally, we get the approximation for the potential $V(\mathbf{r})$ by superposing the uniform electric field and the aforementioned potentials:

$$V(\mathbf{r}) \approx -E_0 z + V_1(\mathbf{r}) + V_2(\mathbf{r}). \quad (14)$$

3.2. Imaging rule for general multipoles. Here, we review Poladian's imaging framework for general multipole sources. We shall consider the case when a multipole source \mathcal{Y}_{lm} is an initial image source. Note that, since the point charge potential G and the dipole potential D satisfy $G(\mathbf{r}) = \frac{1}{4\pi} \mathcal{Y}_{00}$ and $D(\mathbf{r}) = \mathcal{Y}_{10}(\mathbf{r})$, then the image potentials (10) and (11) can be seen as special cases of potentials generated by image multipole sources.

Before considering a general multipole source \mathcal{Y}_{lm} , let us first consider a sectoral multipole $\mathcal{Y}_{|m|,m}$. If an initial sectoral multipole $\mathcal{Y}_{|m|,m}$ is located at $(0, 0, z_0)$, the image sequence is produced by Poladian's rule as follows: $u_m^{(2k)} \mathcal{Y}_{|m|,m}$ at $(0, 0, z_{2k})$ and $-u_m^{(2k+1)} \mathcal{Y}_{|m|,m}$ at $(0, 0, -z_{2k+1})$ for $k = 0, 1, 2, \dots$. Similarly, if an initial location is $(0, 0, -z_0)$, then the following image sequence is produced: $u_m^{(2k)} \mathcal{Y}_{|m|,m}$ at $(0, 0, -z_{2k})$ and $-u_m^{(2k+1)} \mathcal{Y}_{|m|,m}$ at $(0, 0, +z_{2k+1})$ for $k = 0, 1, 2, \dots$. Here, $u_m^{(k)}$ satisfies a recursive relation

$$u_m^{(k+1)} = \tau \left(\frac{R}{d + z_k} \right)^{2|m|+1} u_m^{(k)}, \quad k = 0, 1, 2, \dots$$

It can be explicitly solved as follows:

$$u_m^{(k)} = \tau^k \left(\frac{\sinh(s + t_0)}{\sinh(ks + s + t_0)} \right)^{2|m|+1}.$$

Let U_m^\pm be the potential due to the image sequence when the initial position is $(0, 0, \pm z_0)$, respectively. Then the potential U_m^\pm is given by

$$U_m^\pm(\mathbf{r}) = \sum_{k=0}^{\infty} u_m^{(2k)} \mathcal{Y}_{|m|,m}(\mathbf{r} \mp \mathbf{z}_{2k}) - u_m^{(2k+1)} \mathcal{Y}_{|m|,m}(\mathbf{r} \pm \mathbf{z}_{2k+1}). \quad (15)$$

Now we consider the general multipole source $\mathcal{Y}_{lm}(\mathbf{r})$. Let $U_{l,m}^\pm$ be the potential generated by all the image sources when an initial image multipole \mathcal{Y}_{lm} is located at the center of the sphere B_\pm , respectively. In [4], it was shown that the general multipole \mathcal{Y}_{lm} can be represented as a derivative of the sectoral multipole $\mathcal{Y}_{|m|,m}$:

$$\mathcal{Y}_{lm}(\mathbf{r} \mp \mathbf{r}_0) = \mathcal{D}_{lm}^\pm [\mathcal{Y}_{|m|,m}(\mathbf{r} \mp \mathbf{z}_0)], \quad (16)$$

where the differential operator \mathcal{D}_{lm}^\pm is defined by

$$\mathcal{D}_{lm}^\pm[f] = \frac{(\pm 1)^{l-|m|}}{(l-|m|)! N_{l,m,|m|,m}} \frac{\partial^{l-|m|}}{\partial z_0^{l-|m|}} f \Big|_{z_0=d}.$$

Therefore, the image potential $U_{l,m}^\pm$ is represented as

$$U_{l,m}^\pm(\mathbf{r}) = \mathcal{D}_{lm}^\pm [U_m^\pm(\mathbf{r})]. \quad (17)$$

Actually, this is not the end. We need to be careful when we consider the case $m = 0$. In this case, the total charges on each sphere B_\pm may be non-zero. Since this is unphysical, we have to neutralize them. We introduce an image potential by locating a point charge $-Q_l^\pm$ at the center of the sphere B_\pm , respectively. Here, the constant Q_l^\pm is to be determined. More specifically, we should modify $U_{l,m}^\pm$ as follows:

$$U_{l,m}^\pm(\mathbf{r}) = \mathcal{D}_{lm}^\pm [U_m^\pm(\mathbf{r})] - \delta_{0m} Q_{l,1}^\pm U_0^+(\mathbf{r})|_{z_0=d} - \delta_{0m} Q_{l,2}^\pm U_0^-(\mathbf{r})|_{z_0=d}, \quad (18)$$

where δ_{lm} is the Kronecker delta and the constant $Q_{l,i}^\pm$ is chosen so that the total flux on each surface ∂B_\pm is zero.

4. PROOFS OF THE MAIN RESULTS

Here, we prove our main results.

4.1. From image charges to TO. We prove the following lemma.

Lemma 1. (Connection formula) *The potential $u_k G(\mathbf{r} \mp \mathbf{z}_k)$ generated by the image charges can be rewritten using TO basis as follows: for $\mathbf{r} \in \mathbb{R}^3 \setminus (B_1 \cup B_2)$, we have*

$$u_k G(\mathbf{r} \mp \mathbf{z}_k) = \frac{\sinh(s+t_0)}{4\pi\alpha} \sum_{n=0}^{\infty} [\tau e^{-(2n+1)s}]^k \times e^{-(2n+1)(s+t_0)} \mathcal{M}_{n,\pm}^0(\mathbf{r}). \quad (19)$$

Proof. We have from (1) that

$$z + i\rho = \frac{2\alpha}{e^{\xi-i\eta} - 1} + \alpha.$$

We also have the following identity:

$$\coth t = \frac{\sinh 2t}{\cosh 2t - 1} = \frac{2}{e^{2t} - 1} + 1.$$

Hence, by letting $\mathbf{z}(t) = (0, 0, \alpha \coth t)$, it follows that

$$\begin{aligned} \frac{1}{|\mathbf{r} - \mathbf{z}(t)|} &= |z + i\rho - \alpha \coth t|^{-1} \\ &= \frac{1}{2\alpha} \left| \frac{1}{e^{\xi - i\eta} - 1} - \frac{1}{e^{2t} - 1} \right|^{-1} \\ &= \frac{1}{2\alpha} \left| \frac{(e^{2t} - 1)(e^{\xi - i\theta} - 1)}{e^{2t}(e^{\xi - 2t - i\theta} - 1)} \right|^{-1} \\ &= \frac{\sinh |t|}{\alpha} \frac{\sqrt{\cosh \xi - \cos \eta}}{\sqrt{\cosh(\xi - 2t) - \cos \eta}}. \end{aligned} \quad (20)$$

From (7), it is easy to check that we have

$$\frac{1}{\sqrt{\cosh(\xi - 2t) - \cos \eta}} = \sqrt{2} \sum_{n=0}^{\infty} e^{-(n+\frac{1}{2})|\xi-2t|} P_n(\cos \theta). \quad (21)$$

Then, from (20), we get

$$\begin{aligned} \frac{\alpha}{\sinh |t|} \frac{1}{|\mathbf{r} \mp \mathbf{z}(t)|} &= \sqrt{2} \sqrt{\cosh \xi - \cos \theta} \\ &\times \sum_{n=0}^{\infty} e^{-(2n+1)t} e^{\pm(n+\frac{1}{2})\xi} P_n(\cos \theta). \end{aligned}$$

Therefore, from the fact that $\mathbf{z}_k = \mathbf{z}(ks + s + t_0)$ and the definitions of u_k, G and $\mathcal{M}_{n,\pm}^m$, the conclusion follows immediately. \square

As explained in the main text, by applying the above lemma to (10) and using the following identity

$$\sum_{k=0}^{\infty} [\tau e^{-(2n+1)s}]^k = \frac{e^{(2n+1)s}}{e^{(2n+1)s} - \tau}, \quad (22)$$

we obtain the following result.

Theorem 2. *Let $U(\mathbf{r})$ be defined as in (10). Then $U(\mathbf{r})$ can be rewritten using TO basis as follows:*

$$U(\mathbf{r}) = \frac{\sinh(s + t_0)}{4\pi\alpha} \sum_{n=0}^{\infty} \frac{e^{-(2n+1)t_0}}{e^{(2n+1)s} - \tau} \left(\mathcal{M}_{n,+}^0(\mathbf{r}) - \mathcal{M}_{n,-}^0(\mathbf{r}) \right).$$

4.2. Approximate analytical solution. Now we prove the following result which states an approximate analytical solution for $V(\mathbf{r})$.

Theorem 3. *If $|\tau| \approx 1$, the following approximation for the electric potential $V(\mathbf{r})$ holds: for $\mathbf{r} \in \mathbb{R}^3 \setminus (B_1 \cup B_2)$,*

$$V(\mathbf{r}) \approx -E_0 z + \sum_{n=0}^{\infty} \tilde{A}_n (\mathcal{M}_{n,+}^0(\mathbf{r}) - \mathcal{M}_{n,-}^0(\mathbf{r})),$$

where the coefficient \tilde{A}_n is given by

$$\begin{aligned} \tilde{A}_n &= E_0 \frac{2\tau\alpha}{3 - \tau} \times \frac{2n + 1 - \gamma_0}{e^{(2n+1)s} - \tau}, \\ \gamma_0 &= \sum_{n=0}^{\infty} \frac{2n + 1}{e^{(2n+1)s} - \tau} \bigg/ \sum_{n=0}^{\infty} \frac{1}{e^{(2n+1)s} - \tau}. \end{aligned}$$

Proof. We shall prove the result by applying our connection formula to Poladian's solution. From Theorem 2 and the following identity:

$$\frac{\partial}{\partial z_0} \Big|_{z_0=d} = -\frac{\sinh^2 s}{\alpha} \frac{\partial}{\partial t_0} \Big|_{t_0=0},$$

we get

$$\begin{aligned} V_1(\mathbf{r}) &= p_0 \partial_{z_0} \Big|_{z_0=d} U(\mathbf{r}) \\ &= E_0 \frac{2\tau\alpha}{3-\tau} \sum_{n=0}^{\infty} \frac{2n+1 - \coth s}{e^{(2n+1)s} - \tau} (\mathcal{M}_{n,+}^0(\mathbf{r}) - \mathcal{M}_{n,-}^0(\mathbf{r})). \end{aligned} \quad (23)$$

Similarly, we have

$$V_2(\mathbf{r}) = -QU(\mathbf{r}) \Big|_{z_0=d} = -Q \sum_{n=0}^{\infty} \frac{\mathcal{M}_{n,+}^0(\mathbf{r}) - \mathcal{M}_{n,-}^0(\mathbf{r})}{e^{(2n+1)s} - \tau}. \quad (24)$$

Now let us consider the constant Q . Its expression derived in (13) does not converge for $|\tau| > e^s$. So, here we derive the constant Q in a slightly different way. We impose the following condition:

$$\int_{\partial B_+} \frac{\partial V_1}{\partial \mathbf{n}} dS + \int_{\partial B_+} \frac{\partial V_2}{\partial \mathbf{n}} dS = 0.$$

Then, by using Theorem 9, we obtain

$$E_0 \frac{2\tau\alpha}{3-\tau} \sum_{n=0}^{\infty} \frac{2n+1 - \coth s}{e^{(2n+1)s} - \tau} = Q \sum_{n=0}^{\infty} \frac{1}{e^{(2n+1)s} - \tau}. \quad (25)$$

Hence, we see that

$$Q = \gamma_0 - E_0 \frac{2\tau\alpha}{3-\tau} \coth s.$$

Therefore, from (14), (23) and (24), the conclusion follows. \square

4.3. Electric field at the origin and the polarizability. From (6), we can see that the magnitude of the electric field at the gap is given by

$$E = -(\nabla V \cdot \hat{\mathbf{e}}_z)(0, 0, 0) = E_0 - \frac{2^{3/2}}{\alpha} \sum_{n=0}^{\infty} A_n (2n+1) (-1)^n.$$

As mentioned in the main text, the absorption cross section σ_a is given by $\sigma_a = \omega \text{Im}\{p\}$ where p is the polarizability. In [3], it was shown that the polarizability p is given by

$$p = \sqrt{2}\alpha^2 \sum_{n=0}^{\infty} (2n+1) A_n.$$

Therefore, by replacing A_n by \tilde{A}_n , we can derive approximate analytical expressions for E and σ_a .

4.4. General multipole sources. Here we generalize our connection formula to the case of general multipole source $\mathcal{Y}_{lm}(\mathbf{r})$. As mentioned in the main text, it is essentially used to develop the hybrid numerical scheme for plasmonic spheres.

We first consider the sectoral multipole $\mathcal{Y}_{|m|,m}$. We can represent it using TO basis as follows.

Lemma 4. For $\mathbf{r} \in \mathbb{R}^3 \setminus (B_+ \cup B_-)$ (or $|\xi| < s$), we have

$$u_m^{(k)} \mathcal{Y}_{|m|m}(\mathbf{r} \mp \mathbf{z}_k) = \sum_{n=|m|}^{\infty} g_n^m \lambda_n^m [\tau e^{-(2n+1)s}]^k \\ \times e^{-(2n+1)s} \mathcal{M}_{n,\pm}^m(\mathbf{r}),$$

where λ_n^m and g_n^m are given by

$$\lambda_n^m = [\sinh(s + t_0)]^{2|m|+1} e^{-(2n+1)t_0}, \\ g_n^m = \frac{1}{\alpha^{|m|+1}} \frac{2^{|m|}}{\sqrt{(2|m|)!}} \sqrt{\frac{(n+|m|)!}{(n-|m|)!}}.$$

Proof. For simplicity, we consider only $u_m^{(k)} \mathcal{Y}_{|m|m}(\mathbf{r} - \mathbf{z}_k)$. From (9) and the fact that $\rho = |\mathbf{r} - \mathbf{z}_k| \sin \theta_k$, we have

$$\mathcal{Y}_{|m|m}(\mathbf{r} - \mathbf{z}_k) = \frac{1}{\sqrt{(2|m|)!}} \frac{P_{|m|}^{(|m|)}(\cos \theta_k) e^{im\phi_k}}{|\mathbf{r} - \mathbf{z}_k|^{|m|+1}} \\ = \omega_m \frac{[\sin \theta_k]^{|m|}}{|\mathbf{r} - \mathbf{z}_k|^{|m|+1}} e^{im\phi_k} \\ = \omega_m \frac{\rho^{|m|}}{|\mathbf{r} - \mathbf{z}_k|^{2|m|+1}} e^{im\phi_k}, \quad (26)$$

where the constant ω_m is defined by

$$\omega_m = \frac{(-1)^{|m|} (2|m| - 1)!!}{\sqrt{(2|m|)!}}.$$

From (20) and the fact that $\mathbf{z}_k = \mathbf{z}(ks + s + t_0)$, we see that

$$\frac{1}{|\mathbf{r} \mp \mathbf{z}_k|} = \frac{\sin(ks + s + t_0) \sqrt{\cosh \xi - \cos \eta}}{\alpha \sqrt{\cosh(\xi \mp 2(ks + s + t_0)) - \cos \eta}}.$$

We also have from (2) that $\rho = \alpha \sin \eta / (\cosh \xi - \cos \eta)$. By substituting these expressions for $1/|\mathbf{r} - \mathbf{z}_k|$ and ρ into (26), we get

$$u_m^{(k)} \mathcal{Y}_{|m|m}(\mathbf{r} - \mathbf{z}_k) = \tau^k \frac{\sinh^{2|m|+1}(s + t_0)}{\sqrt{(2|m|)!} \alpha^{|m|+1}} \sqrt{\cosh \xi - \cos \eta} \\ \times \frac{2^{|m|+1/2} (-1)^{|m|} (2|m| - 1)!! [\sin \eta]^{|m|}}{[2(\cosh(\xi - 2(ks + s + t_0)) - \cos \eta)]^{|m|+1/2}}. \quad (27)$$

By letting $t = e^{-|\zeta|}$ and $x = \cos \eta$ in (8), it is easy to check that

$$\frac{(-1)^m (2m - 1)!! [\sin \eta]^m}{[2(\cosh \zeta - \cos \eta)]^{m+1/2}} = \sum_{n=m}^{\infty} e^{-(n+\frac{1}{2})|\zeta|} P_n^m(\cos \eta).$$

By applying this identity to (27), we immediately obtain that

$$u_m^{(k)} \mathcal{Y}_{|m|m}(\mathbf{r} - \mathbf{z}_k) = \tau^k 2^{|m|} \frac{\sinh^{2|m|+1}(s + t_0)}{\sqrt{(2|m|)!} \alpha^{|m|+1}} \\ \times \sqrt{2} \sqrt{\cosh \xi - \cos \eta} \\ \times \sum_{n=|m|}^{\infty} e^{-(2n+1)(ks+s+t_0)} e^{(n+\frac{1}{2})\xi} P_n^{|m|}(\cos \eta),$$

for $|\xi| < s$. Then, from the definition of $\mathcal{M}_{n,+}^m$, the conclusion follows. \square

Now we are ready to prove the connection formula for general multipole sources. We have the following result.

Theorem 5. (Converting multipole images to TO) Assume l and m to be integers such that $l \geq 1$ and $-l \leq m \leq l$. Then the potential U_{lm}^\pm can be rewritten in terms of TO basis as follows: for $\mathbf{r} \in \mathbb{R}^3 \setminus (B_+ \cup B_-)$,

$$\begin{aligned} U_{lm}^\pm(\mathbf{r}) &= \sum_{n=|m|}^{\infty} \frac{g_{lmn}^\pm \mathcal{D}_{lm}[\lambda_n^m]}{e^{2(2n+1)s} - \tau^2} (e^{(2n+1)s} \mathcal{M}_{n,\pm}^m(\mathbf{r}) - \tau \mathcal{M}_{n,\mp}^m(\mathbf{r})) \\ &\quad - \delta_{0m} \frac{\tilde{Q}_{l,1}^\pm}{2} \sum_{n=0}^{\infty} \frac{\mathcal{M}_{n,+}^0(\mathbf{r}) + (-1)^l \mathcal{M}_{n,-}^0(\mathbf{r})}{e^{(2n+1)s} + (-1)^l \tau} \\ &\quad \mp \delta_{0m} \frac{\tilde{Q}_{l,2}^\pm}{2} \sum_{n=0}^{\infty} \frac{\mathcal{M}_{n,+}^0(\mathbf{r}) - (-1)^l \mathcal{M}_{n,-}^0(\mathbf{r})}{e^{(2n+1)s} - (-1)^l \tau}, \end{aligned}$$

where the operator \mathcal{D}_{lm} and the constant $Q_{l,i}^\pm$ are given by

$$\begin{aligned} g_{lmn}^\pm &= \frac{(\pm 1)^{l-|m|}}{\alpha^{|m|+1}} \frac{2^{|m|}}{\sqrt{(2|m|)!}} \sqrt{\frac{(n+|m|)!}{(n-|m|)!}}, \\ N_{lm} &= (l-|m|)! \sqrt{\binom{l+|m|}{l+m} \binom{l+|m|}{|m|+m}}, \\ \tilde{Q}_{l,i}^\pm &= \sum_{n=0}^{\infty} \frac{(\pm 1)^l g_n^0 \mathcal{D}_{l0}^\pm[\lambda_n^0]}{e^{(2n+1)s} - (-1)^{l+i} \tau} \bigg/ \sum_{n=0}^{\infty} \frac{1}{e^{(2n+1)s} - (-1)^{l+i} \tau}. \end{aligned}$$

Proof. By applying Lemma 4 to (15) and then using the following identity:

$$\sum_{k=0}^{\infty} [\tau e^{-(2n+1)s}]^{2k} = \frac{e^{2(2n+1)s}}{e^{2(2n+1)s} - \tau^2}, \quad (28)$$

we obtain

$$U_m^\pm(\mathbf{r}) = \sum_{n=|m|}^{\infty} g_n^m \lambda_n^m \frac{e^{(2n+1)s} \mathcal{M}_{n,\pm}^m(\mathbf{r}) - \tau \mathcal{M}_{n,\mp}^m(\mathbf{r})}{e^{2(2n+1)s} - \tau^2}.$$

Then, by using (18), we get

$$\begin{aligned} U_{l,m}^\pm(\mathbf{r}) &= \sum_{n=|m|}^{\infty} \frac{g_n^m \mathcal{D}_{lm}^\pm[\lambda_n^m]}{e^{2(2n+1)s} - \tau^2} (e^{(2n+1)s} \mathcal{M}_{n,\pm}^m(\mathbf{r}) - \tau \mathcal{M}_{n,\mp}^m(\mathbf{r})) \\ &\quad - \delta_{0m} Q_{l,1}^\pm \frac{\sinh s}{\alpha} \sum_{n=0}^{\infty} \frac{e^{(2n+1)s} \mathcal{M}_{n,+}^0(\mathbf{r}) - \tau \mathcal{M}_{n,-}^0(\mathbf{r})}{e^{2(2n+1)s} - \tau^2} \\ &\quad - \delta_{0m} Q_{l,2}^\pm \frac{\sinh s}{\alpha} \sum_{n=0}^{\infty} \frac{(-\tau) \mathcal{M}_{n,+}^0(\mathbf{r}) + e^{(2n+1)s} \mathcal{M}_{n,-}^0(\mathbf{r})}{e^{2(2n+1)s} - \tau^2}. \end{aligned} \quad (29)$$

Now we consider the following flux conditions:

$$\int_{\partial B_+} \frac{\partial(U_{l,m}^\pm)}{\partial \mathbf{n}} dS = 0, \quad \int_{\partial B_-} \frac{\partial(U_{l,m}^\pm)}{\partial \mathbf{n}} dS = 0. \quad (30)$$

Then, by applying Theorem 9 to the above conditions and using (29), we obtain that

$$Q_{l,1}^\pm \frac{\sinh s}{\alpha} = \frac{\tilde{Q}_{l,1}^\pm \pm \tilde{Q}_{l,2}^\pm}{2}, \quad Q_{l,2}^\pm \frac{\sinh s}{\alpha} = (-1)^l \frac{\tilde{Q}_{l,1}^\pm \mp \tilde{Q}_{l,2}^\pm}{2}. \quad (31)$$

By rearranging terms and using the fact that $N_{lm} = (l - |m|)!N_{l,m,|m|,m}$, the conclusion follows. \square

5. HYBRID NUMERICAL SCHEME FOR MANY SPHERES

In this section, we show that the Cheng and Greengard hybrid method can be extended to systems of plasmonic spheres by using the established connection between the image method and TO.

5.1. Multipole expansion. Suppose that the spheres $B_j, j = 1, 2, \dots, J$ of radius R are located disjointly in \mathbb{R}^3 and let \mathbf{c}_j be the center of the sphere B_j . We also suppose that all the spheres have the same permittivity ϵ and $\epsilon_0 = 1$. The classical way to solve the many-spheres problem is Rayleigh's multipole expansion method. Here, we briefly review this method. Recall that the solid harmonics \mathcal{Y}_{lm} and \mathcal{Z}_{lm} are defined by

$$\mathcal{Y}_{lm}(\mathbf{r}) = \frac{Y_l^m(\theta, \phi)}{r^{l+1}}, \quad \mathcal{Z}_{lm}(\mathbf{r}) = r^l Y_l^m(\theta, \phi).$$

Any solution to Laplace's equation can be represented as a sum of \mathcal{Y}_{lm} and \mathcal{Z}_{lm} . The potential $V(\mathbf{r})$ can be represented as the following multipole expansion: for \mathbf{r} belonging to the region outside the spheres, we have

$$V(\mathbf{r}) = -E_0 z + \sum_{j=1}^J \sum_{l=1}^{\infty} \sum_{m=-l}^l C_{j,lm} \mathcal{Y}_{lm}(\mathbf{r} - \mathbf{c}_j), \quad (32)$$

where the coefficients $C_{j,lm}$ are unknown constants. For the inner region of B_j , we can easily extend the above representation by imposing the continuity of the potential on the surface ∂B_j . For $\mathbf{r} \in B_j$, we have

$$V(\mathbf{r}) = \sum_{l=0}^{\infty} \sum_{m=-l}^l C_{j,lm} \frac{\mathcal{Z}_{lm}(\mathbf{r} - \mathbf{c}_j)}{R^{2l+1}}.$$

Then, by using the addition formula for solid harmonics (see (35)) and the flux boundary conditions, $\nabla V \cdot \mathbf{n}|_{ext} = \epsilon \nabla V \cdot \mathbf{n}|_{int}$ on the surface ∂B_j , the infinite dimensional linear system for unknowns $C_{j,lm}$ can be derived. If all the spheres are well-separated, the linear system can be truncated by a small order. But, if some of the spheres are close to touching, the charge densities on their surfaces become more singular. So more harmonics are required to describe them accurately.

5.2. Cheng and Greengard's hybrid method. Now we briefly review Cheng and Greengard's hybrid method and then explain which part should be modified for systems of plasmonic spheres. To illustrate Cheng and Greengard's method, let us consider an example of three spheres (that is, $J = 3$). Suppose that the spheres B_1 and B_2 are closely located but well-separated from B_3 . Then the charge density on ∂B_3 can be well represented by a low-order spherical harmonics expansion. But the charge densities both on ∂B_1 and ∂B_2 may be singular, so it is better to use the image method to describe their associated potentials. In view of this observation, Cheng and Greengard introduced the modified representation: for \mathbf{r} belongs to the region

outside the spheres,

$$V(\mathbf{r}) = -E_0 z + \sum_{j=1}^2 \sum_{l=1}^{\infty} \sum_{m=-l}^l C_{12,lm} U_{12,lm}(\mathbf{r}) + \sum_{l=1}^{\infty} \sum_{m=-l}^l C_{3,lm} \mathcal{Y}_{lm}(\mathbf{r} - \mathbf{c}_3),$$

where $U_{12,lm}$ is the potential which includes all the image sources induced from the multipoles $C_{j,lm} \mathcal{Y}_{lm}(\mathbf{r} - \mathbf{c}_j)$ for $j = 1, 2$, due to the interaction between two spheres B_1 and B_2 . This representation for $V(\mathbf{r})$ can be directly generalized to a system of arbitrary number of spheres.

As mentioned previously, the image method cannot be applied for plasmonics. So, our strategy for extending the hybrid method to systems of plasmonic spheres is to convert the image series for the multipole sources to a TO-type solution.

5.3. Outline of the modified algorithm. Here, we explain the algorithm of the modified hybrid scheme for the plasmonic spheres.

- 1 Write down the potential $V(\mathbf{r})$ in the multipole expansion form as in (32).
- 2 If a pair of spheres, say B_j and B_k , are closely located (the separating distance is smaller than a given number, for example, the radius R), then we rotate the xyz -axis for both $\mathbf{r} - \mathbf{c}_j$ and $\mathbf{r} - \mathbf{c}_k$ so that the $+z$ -axis is in the direction of the axis of the pair of spheres, that is, $\mathbf{c}_j - \mathbf{c}_k$.
- 3 We also transform the multipole expansion for B_j into the rotated frame using formula (36). Let us denote the coefficients in the rotated frame by $C'_{j,lm}$.
- 4 By using the connection formula for general multipoles (Theorem 5), we modify the multipole expansion in the rotated frame by replacing $C'_{j,lm} \mathcal{Y}_{lm}(\mathbf{r})$ with TO solution $C'_{j,lm} U_{lm}^+(\mathbf{r})$.
- 5 Do the same as in step 4 for B_k with $U_{lm}^-(\mathbf{r})$ instead of $U_{lm}^+(\mathbf{r})$.
- 6 We convert the TO-type expansion for B_j and B_k into the form of multipole expansion using Theorem 8.
- 7 Rotate the axis of the coordinate system and transform the multipole expansions into the original frame.
- 8 Perform steps 2-7 for all the pairs of closely spaced spheres.
- 9 We extend the resulting multipole expansion to the inner regions of B_j for $j = 1, 2, \dots, J$ using Theorem 7.
- 10 By applying the addition formula (35) for \mathcal{Y}_{lm} and \mathcal{Z}_{lm} with the flux boundary conditions, we construct the infinite dimensional linear system for unknowns $C_{j,lm}$.
- 11 We solve the linear system after truncation.

6. USEFUL FORMULAS

Here we collect many useful formulas and outline their proofs.

6.1. Potential inside two spheres. The following theorems are useful for finding the potential inside two spheres when we have an explicit representation in the outside region.

Theorem 6. *Suppose that V satisfies the Laplace equation inside and outside the two spheres B_+ and B_- . We also assume that the potential V is continuous on each surface ∂B_{\pm} . We also assume that, outside the spheres, the potential V is given by*

$$V(\mathbf{r}) = \sum_{n=0}^{\infty} \sum_{m=-n}^n a_{n,+}^m \mathcal{M}_{n,+}^m(\mathbf{r}) + a_{n,-}^m \mathcal{M}_{n,-}^m(\mathbf{r}),$$

for $\mathbf{r} \in \mathbb{R}^3 \setminus (B_+ \cup B_-)$ and some coefficients $a_{n,\pm}^m$. Then the potential $V(\mathbf{r})$ for $\mathbf{r} \in B_\pm$ is given by

$$V(\mathbf{r}) = \sum_{n=0}^{\infty} \sum_{m=-n}^n (a_{n,\pm}^m e^{(2n+1)s} + a_{n,\mp}^m) \mathcal{M}_{n,\mp}^m(\mathbf{r}),$$

for $\mathbf{r} \in B_\pm$.

Proof. It is obvious that the series on the right-hand side satisfies the Laplace equation. Using the following identity:

$$\begin{aligned} \mathcal{M}_{n,+}^m(\mathbf{r})|_{\partial B_\pm} &= \sqrt{2} \sqrt{\cosh \xi - \cos \eta} e^{\pm(n+1/2)s} Y_n^m(\eta, \varphi) \\ &= e^{\pm(2n+1)s} \mathcal{M}_{n,-}^m(\mathbf{r})|_{\partial B_\pm}, \end{aligned}$$

one can easily check the continuity of the potential V on each surface $\partial B_\pm = \{\xi = \pm s\}$. Therefore, the proof is complete. \square

Theorem 7. *Suppose that V satisfies the Laplace equation inside and outside the two spheres B_+ and B_- . We also assume that the potential V is continuous on each surface ∂B_\pm . Furthermore, we assume that, outside the spheres, the potential V is given by*

$$V(\mathbf{r}) = \sum_{l=0}^{\infty} \sum_{m=-l}^l c_{l,m}^+ \mathcal{Y}_{lm}(\mathbf{r} - \mathbf{r}_0) + c_{l,m}^- \mathcal{Y}_{lm}(\mathbf{r} + \mathbf{r}_0),$$

for $\mathbf{r} \in \mathbb{R}^3 \setminus (B_+ \cup B_-)$ and some coefficients $c_{l,m}^\pm$. Then the potential $V(\mathbf{r})$ for $\mathbf{r} \in B_\pm$ is given by

$$V(\mathbf{r}) = \sum_{l=0}^{\infty} \sum_{m=-l}^l \frac{c_{l,m}^+}{R^{2l+1}} \mathcal{Z}_{lm}(\mathbf{r} - \mathbf{r}_0) + \frac{c_{l,m}^-}{R^{2l+1}} \mathcal{Z}_{lm}(\mathbf{r} + \mathbf{r}_0),$$

for $\mathbf{r} \in B_\pm$.

6.2. Multipole expansion of TO solution. When we apply the hybrid numerical scheme, we need to convert TO solution into a multipole expansion.

Let us consider the following general potential W_\pm in the form of TO solution:

$$W_\pm(\mathbf{r}) = \sum_{n=0}^{\infty} \sum_{m=-n}^n a_{n,\pm}^m \mathcal{M}_{n,\pm}^m(\mathbf{r}), \quad (33)$$

for some coefficients $a_{n,\pm}^m$. We want to convert the potential W_\pm into a multipole expansion form:

$$W_\pm(\mathbf{r}) = \begin{cases} \sum_{l=0}^{\infty} \sum_{m=-n}^n c_{l,m}^\pm \mathcal{Y}_{l,m}(\mathbf{r} \mp \mathbf{r}_0), & \mathbf{r} \in \mathbb{R}^3 \setminus B_\pm, \\ \sum_{l=0}^{\infty} \sum_{m=-n}^n d_{l,m}^\pm \mathcal{Z}_{l,m}(\mathbf{r} \mp \mathbf{r}_0), & \mathbf{r} \in B_\pm. \end{cases} \quad (34)$$

where coefficients $c_{l,m}^\pm$ and $d_{l,m}^\pm$ are to be determined.

We have the following result for explicit formulas for $c_{l,m}^\pm$ and $d_{l,m}^\pm$.

Theorem 8. *(Conversion of TO solution into multipole expansion) The multipole coefficients $c_{l,m}^\pm$ are represented in terms of TO coefficients $a_{n,\pm}^m$ as follows:*

$$\begin{cases} c_{l,m}^\pm = 2\alpha R^{2l+1} \sum_{n=|m|}^{\infty} a_{n,\pm}^m g_n^m \mathcal{D}_{lm}^\pm[\lambda_n^m], \\ d_{l,m}^\pm = 2\alpha \sum_{n=|m|}^{\infty} a_{n,\mp}^m e^{-(2n+1)s} g_n^m \mathcal{D}_{lm}^\pm[\lambda_n^m]. \end{cases}$$

In view of (34), the total flux on the surface ∂B_{\pm} is given as

$$\int_{\partial B_{\pm}} \frac{\partial(W_+ + W_-)}{\partial \mathbf{n}} dS = 4\pi c_{0,0}^{\pm}.$$

So, we have the following flux formula from the above theorem.

Theorem 9. (Total flux formula) Let W_{\pm} be the potential given as (33). Then the total flux on the surface ∂B_{\pm} is

$$\int_{\partial B_{\pm}} \frac{\partial(W_+ + W_-)}{\partial \mathbf{n}} dS = 8\pi\alpha \sum_{n=0}^{\infty} a_{n,\pm}^0.$$

6.3. Coordinate transformation: translation and rotation. To apply Rayleigh's multipole expansion method, we need to represent a multipole source in translated or rotated coordinates. The following identities are derived in [4].

Translation:

We have

$$\begin{aligned} \mathcal{Y}_{lm}(\mathbf{r} - \mathbf{r}') &= \sum_{a=0}^{\infty} \sum_{b=-a}^a w_m w_b w_{m-b} \\ &\times N_{lmab} (-1)^{l+a} \mathcal{Z}_{ab}(\mathbf{r}_{<}) \mathcal{Y}_{l+a, m-b}(\mathbf{r}_{>}), \end{aligned} \quad (35)$$

where $\mathbf{r}_{<}$ is the smaller (in magnitude) of \mathbf{r} and \mathbf{r}' and $\mathbf{r}_{>}$ is the larger.

Rotation:

Suppose that the coordinate axes are rotated through Euler angle α, β, γ . The point (θ, ϕ) becomes $(\tilde{\theta}, \tilde{\phi})$. The following result holds:

$$Y_{lm}(\theta, \phi) = \sum_{M=-l}^l w_m w_M D_{mM}^{(l)}(\alpha, \beta, \gamma) Y_{lM}(\tilde{\theta}, \tilde{\phi}), \quad (36)$$

where

$$D_{mM}^{(l)}(\alpha, \beta, \gamma) = e^{-i\alpha + M\gamma} d_{mM}^l(\beta),$$

and

$$\begin{aligned} d_{mM}^l(\beta) &= \cos(\beta/2)^{2l+m-M} \sin(\beta/2)^{M-m} \\ &\times \sum_t \sqrt{\binom{l+m}{t} \binom{l-M}{t} \binom{l+M}{l+m-t} \binom{l-m}{l-M-t}} \\ &\times (-1)^t \tan(\beta/2)^{2t}. \end{aligned}$$

The summation in t is carried over $\max(0, m-M) \leq t \leq \min(l+m, l-M)$.

6.4. Proof of Theorem 8. Let σ_{\pm} be the charge density on the surface ∂B_{\pm} , respectively. Now let us decompose σ_{\pm} using the spherical harmonics $Y_l^m(\theta_{\pm}, \phi_{\pm})$, where $(r_{\pm}, \theta, \pm, \phi_{\pm})$ are the spherical coordinates for $\mathbf{r} \mp \mathbf{r}_0$. Let us write σ_{\pm} as

$$\sigma_{\pm} = \sum_{l=0}^{\infty} \sum_{m=-l}^l \sigma_{lm}^{\pm} Y_{lm}(\theta_{\pm}, \phi_{\pm}).$$

Here, σ_{lm}^{\pm} can be determined using the orthogonality of the spherical harmonics as follows:

$$\sigma_{lm}^{\pm} = \frac{2l+1}{4\pi} \frac{1}{R^2} \int_{\partial B_{\pm}} \sigma_{\pm} \overline{Y_{lm}}(\theta_{\pm}, \phi_{\pm}) dS. \quad (37)$$

To calculate the right-hand side of (37), we need to express σ_{\pm} and $Y_{lm}(\theta_{\pm}, \phi_{\pm})$ in terms of TO harmonics $Y_n^m(\eta, \varphi)$.

First, let us consider σ_{\pm} . Let 'ext'(or 'int') denote the limit from the outside (or inside) the sphere, respectively. It is well-known that the electric field $\mathbf{E} = -\nabla W$ satisfies the following boundary condition on ∂B_{\pm} :

$$\mathbf{E} \cdot \mathbf{n}|_{ext} - \mathbf{E} \cdot \mathbf{n}|_{int} = \sigma_{\pm}, \quad \text{on } \partial B_{\pm},$$

where \mathbf{n} is the outward unit normal vector to ∂B_{\pm} . To use the above condition, we need an explicit expression for W_{\pm} in the region inside the spheres B_{\pm} , respectively. From Theorem 6, we have, for $\mathbf{r} \in B_{\pm}$,

$$W_{\pm}(\mathbf{r}) = \sum_{n=0}^{\infty} \sum_{m=-n}^n a_{n,\pm}^m e^{(2n+1)s} \mathcal{M}_{n,\mp}^m(\mathbf{r}), \quad (38)$$

respectively. So, by using (5), we obtain

$$\begin{aligned} \sigma_{\pm} &= -\frac{\partial W}{\partial \mathbf{n}} \Big|_{\partial B_{\pm}}^{ext} + \frac{\partial W}{\partial \mathbf{n}} \Big|_{\partial B_{\pm}}^{int} \\ &= (2\alpha)^{1/2} [J(\eta)]^{-3/2} \\ &\quad \times \sum_{n,m} a_{n,\pm}^m (2n+1) e^{(n+\frac{1}{2})s} Y_n^m(\eta, \varphi), \end{aligned} \quad (39)$$

where $J(\eta)$ is defined by

$$J(\eta) = \frac{\alpha}{\cosh s - \cos \eta}.$$

Next, let us consider $Y_n^m(\theta_{\pm}, \phi_{\pm})$. From (16) and Lemma 4, we have for $\mathbf{r} \in \partial B_{+}$,

$$\begin{aligned} Y_l^m(\theta_{\pm}, \varphi_{\pm}) &= R^{l+1} \mathcal{Y}_{l,m}(\mathbf{r} \mp \mathbf{r}_0), \\ &= R^{l+1} \mathcal{D}_{lm}^{\pm} [\mathcal{Y}_{|m|,m}(\mathbf{r} \mp \mathbf{z}_0)], \\ &= R^{l+1} (2\alpha)^{1/2} [J(\eta)]^{-1/2} \\ &\quad \times \sum_{n=0}^{\infty} g_n^m \mathcal{D}_{lm}^{\pm} [\lambda_n^m] e^{-(n+1/2)s} Y_n^m(\eta, \varphi). \end{aligned} \quad (40)$$

Now, we are ready to compute σ_{lm}^{\pm} . By substituting (39) and (40) into E(37), we obtain

$$\begin{aligned} \sigma_{lm}^{\pm} &= \frac{2l+1}{4\pi} \frac{1}{R^2} \int_0^{2\pi} \int_0^{\pi} \sigma_{\pm} \overline{Y_{lm}} [J(\eta)]^2 \sin \eta d\eta d\varphi, \\ &= (2l+1) 2\alpha R^{l-1} \sum_{n=|m|}^{\infty} a_{n,\pm}^m g_n^m \mathcal{D}_{lm}^{\pm} [\lambda_n^m]. \end{aligned} \quad (41)$$

It is easy to check that the potential generated by the charge densities $\sigma_{\pm} = \sum \sigma_{lm}^{\pm} Y_{lm}$ is given as follows: for $\mathbf{r} \in \mathbb{R}^3 \setminus (B_{+} \cup B_{-})$,

$$W_{\pm}(\mathbf{r}) = \sum_{l,m} \sigma_{lm}^{\pm} \frac{R^{l+2}}{2l+1} \mathcal{Y}_{lm}(\mathbf{r} \mp \mathbf{r}_0)$$

By comparing the above expression and (34), we immediately arrive at

$$c_{l,m}^{\pm} = \sigma_{lm}^{\pm} \frac{R^{l+2}}{2l+1}.$$

Then, the formula for $c_{l,m}^{\pm}$ follows from (41). For the case of $d_{l,m}^{\pm}$, it can be proved in a similar way. \square

REFERENCES

- [1] H. Cheng and L. Greengard, A method of images for the evaluation of electrostatic fields in systems of closely spaced conducting cylinders, *SIAM Appl. Math.*, 58 (1998) 121-141.
- [2] H. Cheng, On the method of images for systems of closely spaced conducting spheres, *SIAM Appl. Math.*, 61 (2000) 1324-1337.
- [3] A. Goyette and A. Navon, Two dielectric spheres in an electric field, *Phys. Rev. B* 13 (1976) 4320-4327.
- [4] L. Poladian, *Effective Transport and Optical Properties of Composite Materials*, Ph.D. thesis, University of Sydney, 1990.
- [5] L. Poladian, General theory of electrical images in sphere pairs, *Q. J. Mech. Appl. Math.* 41 (1988), 395-417.
- [6] L. Poladian, Asymptotic behaviour of the effective dielectric constants of composite materials, *Proc. Roy. Soc. A* 426 (1988), 343-359.

DEPARTMENT OF MATHEMATICS, ETH ZÜRICH, RÄMISTRASSE 101, CH-8092 ZÜRICH, SWITZERLAND

E-mail address: sanghyeon.yu@math.ethz.ch

DEPARTMENT OF MATHEMATICS, ETH ZÜRICH, RÄMISTRASSE 101, CH-8092 ZÜRICH, SWITZERLAND

E-mail address: habib.ammari@math.ethz.ch